Ann Nucl Med (2015) 29:84–90
DOI 10.1007/s12149-014-0918-6

ORIGINAL ARTICLE

Distribution of residual long-lived radioactivity in the inner concrete walls of a compact medical cyclotron vault room

Toshioh Fujibuchi · Akihiro Nohtomi · Shingo Baba · Masayuki Sasaki · Isao Komiya · Yoshiyuki Umedzu · Hiroshi Honda

Received: 25 March 2014 / Accepted: 30 September 2014 / Published online: 14 October 2014

Abstract
Objective Compact medical cyclotrons have been set up to generate the nuclides necessary for positron emission tomography. In accelerator facilities, neutrons activate the concrete used to construct the vault room; this activation increases with the use of an accelerator. The activation causes a substantial radioactive waste management problem when facilities are decommissioned. In the present study, several concrete cores from the walls, ceiling and floor of a compact medical cyclotron vault room were samples 2 years after the termination of operations, and the radioactivity concentrations of radionuclides were estimated.
Methods Cylindrical concrete cores 5 cm in diameter and 10 cm in length were bored from the concrete wall, ceiling and floor. Core boring was performed at 18 points. The gamma-ray spectrum of each sample was measured using a high-purity germanium detector. The degree of activation of the concrete in the cyclotron vault room was analyzed, and the range and tendency toward activation in the vault room were examined.
Results ^{60}Co and ^{152}Eu were identified by gamma-ray spectrometry of the concrete samples. ^{152}Eu and ^{60}Co are produced principally from the stable isotopes of europium and cobalt by neutron capture reactions. The radioactivity concentration did not vary much between the surface of the concrete and at a depth of 10 cm. Although the radioactivity concentration near the target was higher than the clearance level for radioactive waste indicated in IAEA RS-G-1.7, the mean radioactivity concentration in the walls and floor was lower than the clearance level.
Conclusion The radioactivity concentration of the inner concrete wall of the medical cyclotron vault room was not uniform. The areas exceeding the clearance level were in the vicinity of the target, but most of the building did not exceed the clearance levels.

Keywords Compact medical cyclotron · Radioactivity concentration · Concrete wall · Neutron activation · Clearance level

T. Fujibuchi (✉) · A. Nohtomi · M. Sasaki
Medical Quantum Science, Department of Health Sciences, Faculty of Medical Sciences, Kyushu University Graduate School of Medical Sciences, 3-1-1 Maidashi, Higashi-ku, Fukuoka 812-8582, Japan
e-mail: fujibuch@hs.med.kyushu-u.ac.jp

S. Baba · H. Honda
Department of Clinical Radiology, Graduate School of Medical Sciences, Kyushu University, 3-1-1 Maidashi, Higashi-ku, Fukuoka 812-8582, Japan

I. Komiya · Y. Umedzu
Department of Medical Technology, Kyushu University Hospital, 3-1-1 Maidashi, Higashi-ku, Fukuoka 812-8582, Japan

Introduction

Compact medical cyclotrons have been set up to generate the nuclides necessary for positron emission tomography (PET). In these cyclotrons, the target is irradiated with accelerated protons and deuterons, and positron-emitting radionuclides are generated by the ensuing nuclear reactions. As a result of these reactions, neutrons diffuse into the cyclotron vault room even if the device exhibits no beam loss. Neutrons easily activate the materials used to construct the vault through nuclear reactions. In accelerator facilities, neutrons activate the concrete used to construct the vault room; this activation increases with the use of an accelerator. The activation causes a substantial radioactive

waste management problem when facilities are decommissioned [1]. Several studies on the radioactivity concentration of induced radionuclides in concrete samples have been published, including those for a 1.3-m sector-focusing cyclotron [2], 40-MeV cyclotron [3], 1.3-GeV electron synchrotron [4, 5], a 12-GeV proton synchrotron accelerator [6] and compact medical cyclotron [7, 8]. The use of compact medical cyclotrons has become widespread in Japan since 2002, when the public medical insurance system began to cover fluorodeoxyglucose-PET (FDG-PET) examinations for some types of cancer.

The International Atomic Energy Agency (IAEA) has published a safety guide (RS-G-1.7), in which it has defined the clearance levels (CLs; defined as the radioactivity concentration that would not cause an effective dose exceeding 10 μSv/year) [9]. In Japan, CLs defined in the IAEA RS-G-1.7 have been adopted to ascertain whether to treat decommissioned materials as radioactive waste.

Neutrons produced in the cyclotrons not equipped with self-shields are expected to extend to the entire room in which the cyclotron is housed. Therefore, there is a possibility that the entire concrete wall may be activated. However, the distribution of neutrons is not uniform within the vault room [10]. Therefore, the level of activation may vary in different places. The literature on decommissioning cyclotron facilities is still limited [11]. In addition, there have been no reports describing the radioactivity concentrations of an entire cyclotron vault room, including the floor, walls, and ceiling. In the future, many facilities in which cyclotrons have been installed will be decommissioned due to the aging of equipment. Therefore, it is necessary to accumulate information on the decommissioning of such facilities.

In the present study, several concrete cores from the walls, ceiling and floor of a compact medical cyclotron vault room were sampled, and the radioactivity concentrations of radionuclides were estimated. The degrees of activation of the concrete in the cyclotron vault room were analyzed, and the range and tendency toward activation in the vault room were examined.

Materials and methods

Description of the cyclotron and vault room

The cyclotron was a BC1710 made by Japan Steel Works, Ltd and had been operated for 27 years, from March 1983 to June 2009, in Kyushu University Hospital. The accelerated particles were protons and deuterons; the maximum energy of protons was 17 MeV, and the maximum energy of deuterons was 10 MeV. The mean beam current for both protons and deuterons was 20.7 μA, and the mean beam time per year for the production of radionuclides was approximately 200 h. Table 1 shows the PET isotopes, nuclear reactions, and record of cyclotron operations at the hospital. The concrete core assays were performed in October 2011. The cooling period was, therefore, 2 years and 4 months. The cyclotron was housed in a concrete vault with dimensions of 5.3 m × 5.8 m at the floor, and a height of 3.7 m. The vault was made of concrete; the walls were 52, 52, 130 and 150 cm in thickness, the ceiling was 130 cm thick and the floor was 200 cm thick.

Table 1 The PET isotopes' nuclear reactions and the record of operations

Nuclear reaction	Number of operations per year (*n*/year)	Beam time per year (h/year)	Average beam current (μA)
$^{14}N(p, \alpha)^{11}C$	23.6	12.0	34.1
$^{16}O(p, \alpha)^{13}N$	0.9	0.2	3.7
$^{14}N(d, n)^{15}O$	125.8	88.5	12.3
$^{18}O(p, n)^{18}F$	29.3	46.6	36.4
$^{20}Ne(d, \alpha)^{18}F$	57.8	60.5	25.7

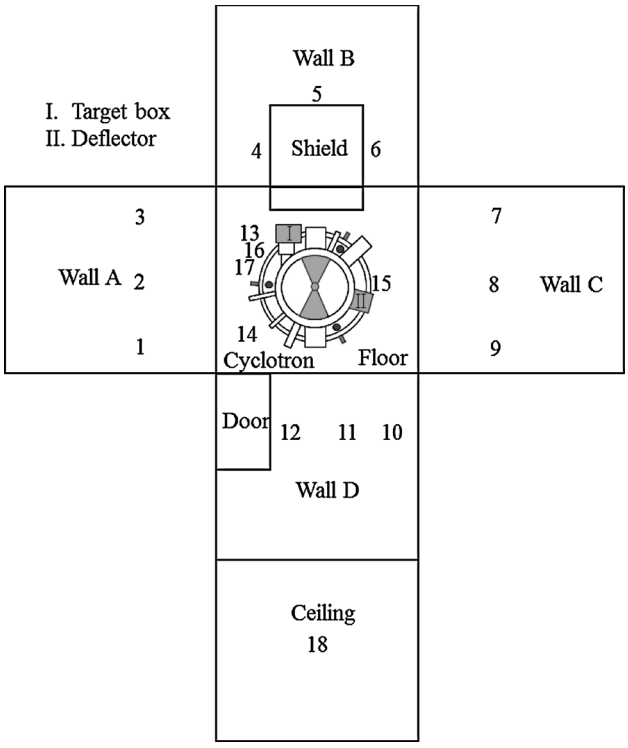

Fig. 1 The development diagram of the cyclotron vault room indicating the sampling points in the walls, ceiling and floor

Table 2 The distance from the target to each concrete core sampling point

Sample ID	Location	Distance from target (cm)	Sample ID	Location	Distance from target (cm)
1	Wall A	325	10	Wall D	578
2	Wall A	258	11	Wall D	531
3	Wall A	212	12	Wall D	465
4	Wall B	195	13	Floor	145
5	Wall B	218	14	Floor	323
6	Wall B	248	15	Floor	277
7	Wall C	338	16	Floor	160
8	Wall C	410	17	Floor	185
9	Wall C	525	18	Ceiling	290

Concrete core sampling

Cylindrical concrete cores 5 cm in diameter and 10 cm in length were bored from the concrete wall, ceiling and floor. Core boring was performed at 18 points. The development diagram and sampling points are shown in Fig. 1. The distances from the target to each sampling point are shown in Table 2. Each concrete core was cut into two 5-cm-thick samples.

Measurements and analysis

The gamma-ray spectrum of each sample was measured using a high-purity germanium detector (ORTEC, model GEM35190). The measurement time was 30,000 s for each sample. In addition, the dose-equivalent rate of each sample was measured using a NaI scintillation survey meter (Aloka, model TCS-171), and the surface concentration density was measured using a Geiger–Muller (GM) survey meter (Aloka, model TGS-136). These measurements and the radionuclide analysis of each sample were performed by the Chiyoda Technology Corporation.

Results

Residual long-lived radionuclides in concrete samples

Figure 2 shows the measured gamma-ray spectrum of the concrete sample (5–10 cm of ID 16) and the background. The primary nuclides detected were ^{60}Co and ^{152}Eu. Each forecast nuclear reaction is shown in Table 3 [12]. ^{152}Eu and ^{60}Co are principally produced from the stable isotopes of europium and cobalt by neutron capture reactions [13, 14]. Figure 3 shows the radioactivity concentration of ^{60}Co and ^{152}Eu in the cores taken at each measurement point.

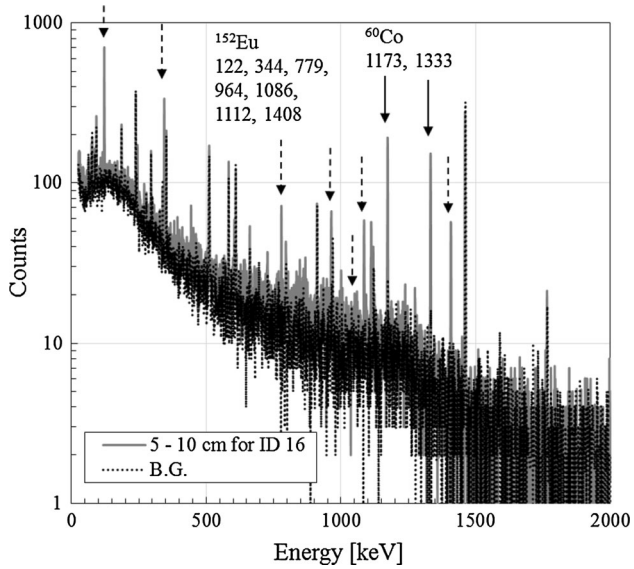

Fig. 2 The energy spectra of representative concrete sample (5–10 cm for ID 16) and the background measured by the germanium detector. The peaks of ^{60}Co are shown with *solid arrows*, and the peaks of ^{152}Eu with *dashed arrows*

Table 3 The activated radionuclides and the nuclear reactions that produce them [12]

Nuclide	Half-life (years)	Reaction	Thermal neutron capture cross-section (barn)	Clearance level (Bq/g)
^{60}Co	5.271	^{59}Co (n, γ)	37	0.1
^{152}Eu	13.537	^{151}Eu (n, γ)	5,900	0.1

The radioactivity concentrations of the samples taken in the vicinity of the target were high (IDs 4, 13, 16, and 17). In the samples (IDs 17 and 18) taken in the vicinity of the target, the radioactivity concentration at a depth of 5 cm was twice as high or higher than the radioactivity concentration at the surface. Differences by depth were not seen in the samples taken at other measurement points, and in half of the samples, the radioactivity concentration at the surface was higher than that at 5–10 cm from the surface (IDs 2, 3, 4, 5, 6, 7, and 9). The radioactivity concentration of the samples taken in the vicinity of the deflector was low (ID 15).

Figure 4 shows the sum of the ratio of the specific activity of each radionuclide to its CL ($\Sigma D/C$: D/C, where D is the specific activity of a radionuclide in the component and C is the CL of the radionuclide) for each concrete sample. Most of the $\Sigma D/C$ values of the concrete core samples fell below one. The $\Sigma D/C$ levels at three points

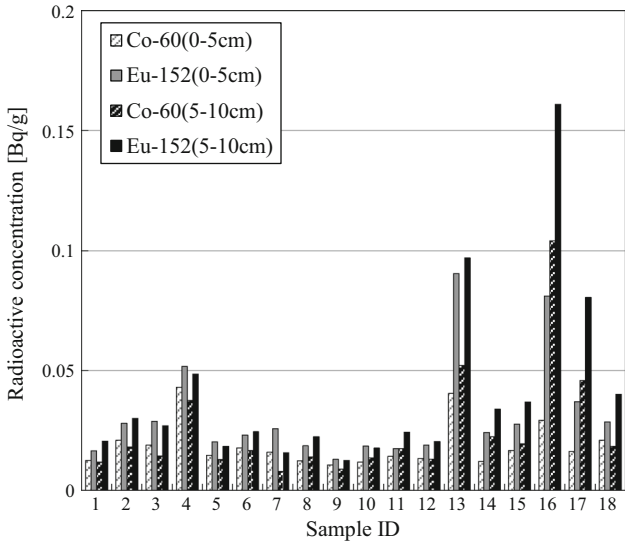

Fig. 3 The radioactivity concentrations of the radionuclides in each concrete core sample

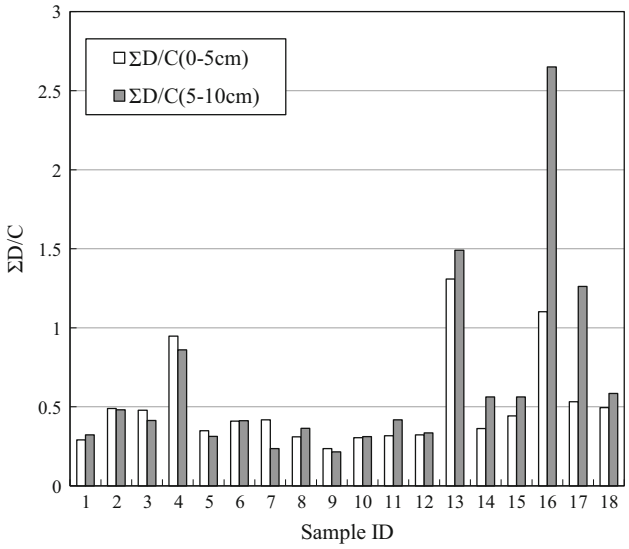

Fig. 4 The sum of the ratios of the specific activity of each radionuclide to the clearance level in each concrete core sample

(IDs 13, 16, and 17) exceeded one. These points were in the vicinity of the target.

The ratios of the radioactivity concentrations of samples from 5–10 cm to 0–5 cm were approximately the same. However, the ratios of two samples (IDs 16 and 17) in the vicinity of the target were more than two.

Based on these data, 6 years after the termination of operations, the Σ*D*/*C*s would be less than one, excluding sample ID 13. The maximum value of the dose-equivalent rate, measured using an NaI scintillation survey meter, was

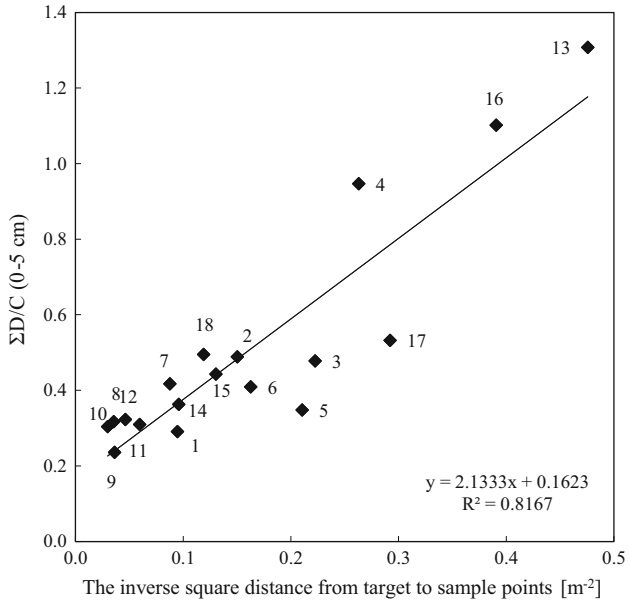

Fig. 5 The relationship between the inverse square distance from the target to the sample points and the Σ*D*/*C* (0–5 cm). The *labels* for each plot are the sample ID

0.02 μSv/h. Most of the dose-equivalent rate measurements were below the detection limit. The surface radioactivity concentration measurements of all samples, taken using a GM survey meter, were below the limit of detection.

Figure 5 shows the relationship between the inverse square distance from the target to the sample points and the Σ*D*/*C* at 0–5 cm. The correlation coefficient of the linear regression line between the Σ*D*/*C* and the inverse square distance from the target was 0.8167.

Discussion

Detected radionuclides

In this study, ^{60}Co and ^{152}Eu were detected. In other studies, ^{46}Sc ($T_{1/2}$ = 83.79 days), ^{65}Zn ($T_{1/2}$ = 243.67 days), ^{134}Cs ($T_{1/2}$ = 2.07 years), ^{22}Na ($T_{1/2}$ = 2.60 years), and ^{54}Mn ($T_{1/2}$ = 312.03 days) have also been detected [3, 7, 8]. In this study, we consider that the reason for the detection of primarily ^{60}Co and ^{152}Eu may be the long cooling time (2.4 years). Over this period of time, the radioactivity concentration of most of the induced radionuclides was attenuated, except for the radionuclides with long half-lives. The present results confirm that the cooling time skews the residual radioactivity concentration toward the long-lived radionuclides. Kimura et al. [3] and Martínez-Serrano et al. [8] previously estimated the specific activity of activation products, and found that ^{46}Sc showed high activity. Since the half-lives of ^{46}Sc, ^{65}Zn and ^{54}Mn

Table 4 The atomic composition of cobalt and europium in concrete (ppm) [8, 13–16]

	Cobalt	Europium
Martínez-Serrano et al. [8]	480	7.7
Suzuki et al. [13]	21.9	1.08
Aggregate	23.5 (0.048–126)	1.07 (0.010–11.2)
Cement	11.9 (0.861–52.3)	1.15 (0.264–4.63)
Kinno et al. [14]		
Ordinary concrete	8–30	0.7–1
Shielding concrete	1–300	0.08–0.4
Low-activation concrete	0.1–1	0.004–0.08
Carrol et al. [15]	2.54	0.294
NUREG/CR-3474 [16]		
Bioshield	9.8 ± 10.3 (1.1–31.0)	0.55 ± 0.38 (0.11–1.2)

are less than only 1 year, the activity would have decayed to 25 % after the 2-year cooling time. A long cooling time can, therefore, be reasonable to help avoid the unnecessary exposure of decommissioning workers. Supporting our findings, other studies showed that the two radioisotopes, ^{60}Co and ^{152}Eu, occupy the main residual radioactivity in terms of the CL value induced in the concrete at the time of decommissioning [13, 14].

The concentration data regarding cobalt and europium in the concrete are valuable, because these concentrations substantially influence the amount of activation. The atomic composition of cobalt and europium in the concrete is shown in Table 4 [8, 13–16]. As shown in the table, "ordinary concrete" is made from aggregates and Portland cement, whereas "shielding concrete" is made from special aggregates for use as radiation shielding, in addition to ordinary Portland cement. The differences in the composition of both cobalt and europium were more than three digits (cobalt; from 0.1 to 480 ppm, europium; from 0.004 to 1.07 ppm). The concentrations of cobalt and europium in the low-activation concretes were about 1/300 to 1/30 of levels in the ordinary concrete [14]. Therefore, based on these data, the estimation of the concentrations of cobalt and europium in the materials used at each facility is important. However, the composition of cobalt and europium could not be measured in this study because the vault room had already been decommissioned, which is a limitation of the study.

Range of activation in the cyclotron vault room

The radioactivity concentration of the radionuclides present in each sample spanned a tenfold range (Fig. 2). The radioactivity concentration is proportional to the neutron fluence generated by the driving time of the cyclotron. In a previous study that evaluated the neutron distribution in a cyclotron vault room using an activation detector, it was confirmed that the neutron fluence in the vicinity of the target was high [11]. The target produced neutrons when the positron nuclide was generated; and therefore, the radioactivity concentration in the concrete was high in the vicinity of the target.

Based on Fig. 5 in the present study, we consider that the amount of activation depends on the distance from the target, because the target is the primary source of neutrons. However, the $\Sigma D/C$s of some samples were far away from the linear regression line reported in Fig. 5, which we believe was due to the following reasons. First, the polyethylene used for neutron shielding of the target box was not uniform in all directions. When the neutron shielding is uniform, the values of $\Sigma D/C$ fall on the regression line. If the shielding is thin, the value of $\Sigma D/C$ is higher than the regression line. If the shielding is thick, the value of $\Sigma D/C$ is lower than the regression line. ID 4 was near the rear side of the target on the beam line extension. There was a target changer behind the target. Because there was no shield behind the target, the $\Sigma D/C$ of ID 4 shifted above the regression line. On the other hand, ID 17 had thick shielding. Therefore, the $\Sigma D/C$ of ID 17 shifted below the regression line.

Second, neutrons are produced by all locations except at the target position. Neutrons are produced in nuclear reactions involving several materials and components of the cyclotron, including the target material, the components of the target assembly (e.g., the body enclosing the target material or the target foils), the collimator system of the cyclotron, and other structures of the cyclotron that may be hit by tails of the beam or by stray ions [20]. Finally, neutrons are scattered in the vault room. The fast neutrons are slowed down via multiple scattering events within the shielding, and 10 % of them are reflected back toward the cyclotron [21].

As shown in Fig. 4, the radioactivity concentration at the depth of 5–10 cm was higher than that at the depth of 0–5 cm in the vicinity of the target, because the neutron energy is different at each measurement point. Thermal neutrons contribute to the activation of the concrete (Table 3). According to previous studies that evaluated the neutron energy in the cyclotron vault room, the neutron energy generated by the nuclear reaction with the target is a continuous spectrum with a peak at 1 MeV, and the thermal neutron component is small [17–19]. In the vicinity of the target, fast neutrons are the main component at the surface of the concrete. These fast neutrons are moderated in the concrete, and the activation peak was observed at a point deep in the concrete. In contrast, in cases where the distance from the target was large, the

thermal neutrons were the main component, because fast neutrons scattered off the wall and floor. Therefore, the surface of the concrete was activated at these points. The literature reports on other facilities [7] and the results of Monte Carlo calculations [8] showed that the peak of activation was at a depth of approximately 10 cm from the concrete surface. Therefore, the evaluation of the radioactivity concentration at approximately 10 cm from the surface of the concrete is not considered to be an undervaluation.

According to the results of this estimate, the radioactivity concentration at the surface of concrete samples exceeded the CLs only in the vicinity of the target. However, the radioactivity concentration was lower than CLs when these values were averaged with those of the concrete in the entire building. It is important to accumulate such data and to obtain a consensus between cyclotron manufacturers, construction companies, PET centers, and regulatory authorities.

In Japan, many institutions use only proton beams [10]. In contrast, the data evaluated in this study also concerned the deuteron beam. Therefore, the amount of neutrons may be different. Gallerani et al. [20] compared the neutron dose from $^{18}O(p, n)^{18}F$, $^{16}O(p, \alpha)^{13}N$, $^{20}Ne(d, \alpha)^{18}F$ and $^{14}N(p, \alpha)^{11}C$ nuclear reactions at 11 points in a non-self-shielded cyclotron room. The normalized yields were 240–380 mSv/μA h for $^{18}O(p, n)^{18}F$, 10–80 mSv/μA h for $^{16}O(p, \alpha)^{13}N$, 20–130 mSv/μA h for $^{20}Ne(d, \alpha)^{18}F$ and 30–110 mSv/μA h for $^{14}N(p, \alpha)^{11}C$. Mukherjee et al. [22] measured the neutron and gamma dose rates of $^{18}O(p, n)^{18}F$, $^{16}O(p, \alpha)^{13}N$, $^{14}N(p, \alpha)^{11}C$ and $^{14}N(d, n)^{15}O$ reactions in a self-shielded cyclotron room. The neutron dose rates were 0.021 μSv/h for $^{18}O(p, n)^{18}F$ and 0.027 μSv/h for $^{16}O(p, \alpha)^{13}N$, whereas the $^{14}N(d, n)^{15}O$ and $^{14}N(p, \alpha)^{11}C$ reactions were not detected. Based on these results, it appears that the most intense neutron dose field was generated in the $H_2^{18}O(p, n)^{18}F$ reaction. The neutron dose, therefore, does not depend on the accelerated particle, but on the kind of nuclear reaction and the material of the target.

The cyclotron used in this study was a positive hydrogen ion type. The negative hydrogen ion-type cyclotron has recently become popular [10, 23]. In this type of cyclotron, the negative hydrogen ions are produced by an external multi-cusp arc discharge ion source producing H- and D-beams. The use of an external source avoids the vacuum problems leading to beam losses and the activation of cyclotrons with internal sources. Furthermore, the negative hydrogen ion-type cyclotron does not require a deflector, which is another source of neutron producing reactions [23]. This reduces beam losses and implies a lower activation of the cyclotron and vault room.

Approaches to reduce activation

An effective way to evaluate the activation condition of the vault before decommissioning would be to assess the neutron distribution in the cyclotron room while the cyclotron is operating. The activation depends on the amount of neutrons. Therefore, neutron shielding strictly in the vicinity of the target is a very effective measure against indoor activation.

When generating positron nuclides with a cyclotron, the number of neutrons generated varies by several folds depending on the target material and the nuclear reactions involved [20, 22, 24]. There is also a possibility that the composition of the concrete may change depending on the geographical region. Therefore, when cyclotron facilities are decommissioned, each facility must sample several concrete cores and evaluate the radioactivity concentration of radionuclides within each of them. To reduce the radioactivity induced in the concrete, a concrete with low-activation potential has been developed, and some facilities have installed concrete with low cobalt and europium concentrations to help prevent activation [14]. Based on the findings of the present study, we established that using low-activation concrete as the floor material right below the target would be an effective approach for reducing activation, thus decreasing the decommissioning costs.

Conclusion

The radioactivity concentration of radionuclides induced in the concrete of a vault room containing a cyclotron that had stopped operating was evaluated. The radioactivity concentration was low in areas away from the target. Near the target, the maximum value of the radioactivity concentration at a depth of 5–10 cm was higher than that at the surface. In contrast, the activity on the surface was higher than that below the surface in areas away from the target. The radioactivity concentration, therefore, differs according to the location of the concrete relative to the target. When decommissioning a cyclotron vault room, it is necessary to evaluate the radioactivity concentration at several points. The areas that exceed the clearance level are likely to be in the vicinity of the target, but the average of the entire building did not exceed the CLs.

References

1. International Atomic Energy Agency. Decommission of small medical, industrial and research facilities. Technical Reports Series No. 44. IAEA (2003).

2. Phillips AB, Prull DE, Ristinen RA, Kraushaar JJ. Residual radioactivity in a cyclotron and its surroundings. Health Phys. 1986;51:337–42.
3. Kimura K, Ishikawa T, Kinno M, Yamadera A, Nakamura T. Residual long-lived radioactivity distribution in the inner concrete wall of a cyclotron vault. Health Phys. 1994;67:62131.
4. Masumoto K, Toyoda A, Eda K, Izumi Y, Shibata T. Evaluation of radioactivity induced in the accelerator building and its application to decontamination work. J Radioanal Nucl Chem. 2003;255:465–9.
5. Saito K, Tanosaki T, Fujii H, Miura T. Analysis of induced radionuclides in low-activation concrete (limestone concrete) using the 12 GeV proton synchrotron accelerator facility at KEK. Radiat Prot Dosim. 2005;116:647–52.
6. Numajiri M. Evaluation of the radioactivity of the pre-dominant gamma emitters in components used at high-energy proton accelerator facilities. Radiat Prot Dosim. 2007;123:417–25.
7. Yamaguchi I, Kimura K, Fujibuchi T, Takahashi Y, Saito K, Otake H. Radiation safety management of residual long-lived radioactivity distributed in an inner concrete wall of a medical cyclotron room. Radiat Prot Dosim. 2011;146:167–9.
8. Martínez-Serrano JJ, Ríos AD. Prediction of neutron induced radioactivity in the concrete walls of a PET cyclotron vault room with MCNPX. Med Phys. 2010;37:6015–21.
9. International Atomic Energy Agency. Application of the concepts of exclusion, exemption and clearance. Safety guide No. RS-G-1.7. IAEA (2004).
10. Fujibuchi T, Yamaguchi I, Watanabe H, Kimura K, Tanaka S, Kida T, et al. Nationwide survey on the operational status of medical compact cyclotrons in Japan. Radiol Phys Technol. 2009;2:126–32.
11. Fujibuchi T, Yamaguchi I, Kasahara T, Iimori T, Masuda Y, Kimura K, et al. Measurement of thermal neutron fluence distribution with use of ^{23}Na radioactivation around a medical compact cyclotron. Radiol Phys Technol. 2009;2:159–65.
12. Radioisotope Pocket Data Book 11th Edition, The Japan Radioisotope Association; 2011.
13. Suzuki A, Iida T, Moriizumi J, Sakuma Y, Takada J, Yamasaki K, Yoshimoto T. Trace element with large activation cross section in concrete materials in Japan. J Nucl Sci Technol. 2001;38:542–50.
14. Kinno M, Kimura K, Nakamura T. Raw materials for low-activation concrete neutron shields. J Nucl Sci Technol. 2002;39:1275–80.
15. Carroll LR. Predicting long-lived, neutron-induced activation of concrete in a cyclotron vault. AIP Conf Proc. 2001;576:301–4.
16. Evans JC, Lepel EL, Sanders RW, Wilkerson CL, Silker W, Thomas CW, et al. Long-lived activation products in reactor materials. NUREG/CR-3474; 1984.
17. Vega-Carrillo HR. Neutron energy spectra inside a PET cyclotron vault room. Nucl Instr Methods A. 2001;463:375–86.
18. Fernandez F, Amgarou K, Domingo C, Garcia MJ, Quincoces G, Marti-Climent JM, et al. Neutron spectrometry in a PET cyclotron with a Bonner sphere system. Radiat Prot Dosim. 2005;126:371–5.
19. Mendez R, Iniguez MP, Martí-Climent JM, Penuelas I, Vega-Carrillo HR, Barquero R. Study of the neutron field in the vicinity of an unshielded PET cyclotron. Phys Med Biol. 2005;50:5141–52.
20. Gallerani R, Cicoria G, Fantuzzi E, Marengo M, Mostacci D. Neutron production in the operation of a 16.5 MeV PETrace cyclotron. Prog Nucl Energy. 2008;50:939–43.
21. Kaur A, Sharma S, Mittal BR. Radiation surveillance in and around cyclotron facility. Indian J Nucl Med. 2012;27:243–5.
22. Tochon-Danguy H, Sachinidis JI, U P, Egan G, Mukherjee B. Occupational radiation exposure at the self-shielded IBA Cyclone 10/5 Cyclotron of the A&R MC, Melbourne, Australia. In: Proceedings of the 15th international conference on cyclotrons and their applications. 1998; p. 105–7.
23. Stevenson NR. Future cyclotron systems: an industrial perspective. In: Proceedings of the 14th international conference on cyclotrons and their applications. 1995; p. 581–4.
24. Ogata Y, Ishigure N, Mochizuki S, Ito K, Hatano K, Abe J, et al. Distribution of thermal neutron flux around a PET cyclotron. Health Phys. 2011;100:S60–6.